

FIG. 1. The number-number pair distribution function $g_{NN}(r)=g_{00}(r)$ for a polydisperse colloidal monolayer with repulsive DLVO potential at density $\rho\bar{\sigma}^2=0.15$. The size dispersion of the colloidal spheres in descending order of the first peak is $s_\sigma=0, 0.2$, and 0.3 .

which will be used to characterize the suspensions and define the parameter α . The orthonormal polynomials satisfying Eq. (8) for the Schulz distribution $f(\sigma)$ are

$$p_j(\sigma)=\left[\frac{j!\Gamma(\alpha+1)}{\Gamma(j+\alpha+1)}\right]^{1/2}L_j^{(\alpha)}\left((\alpha+1)\frac{\sigma}{\bar{\sigma}}\right), \quad (33)$$

where the $L_j^{(\alpha)}(t)$ are the associated Laguerre polynomials.

We present first the results for the repulsive DLVO potential. Computed thermodynamic values are shown in Table I for $\rho\bar{\sigma}^2=0.05, 0.10, 0.15$ and three Schulz distributions of

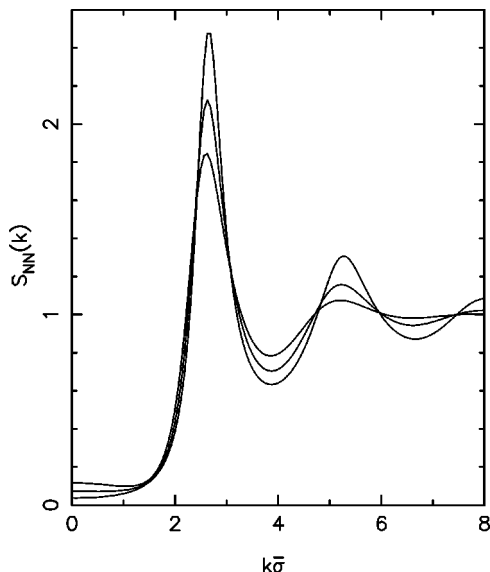


FIG. 2. The number-number structure factor $S_{NN}(k)=1+\rho\tilde{h}_{00}(k)$ for a polydisperse colloidal monolayer with repulsive DLVO potential at density $\rho\bar{\sigma}^2=0.15$. The size dispersion of the colloidal spheres in descending order of the first peak is $s_\sigma=0, 0.2$, and 0.3 . The value at $k=0$ is largest for $s_\sigma=0.3$.

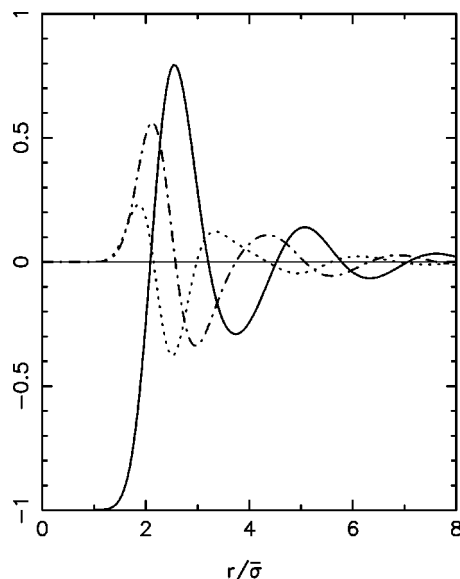


FIG. 3. Pair correlation function coefficients $g_{00}(r)-1$ (solid line), $g_{10}(r)$ (dash-dot line), and $g_{11}(r)$ (dotted line) for a polydisperse colloidal monolayer with repulsive DLVO potential at density $\rho\bar{\sigma}^2=0.15$ and size dispersion $s_\sigma=0.3$.

increasing width, $s_\sigma=0.1, 0.2, 0.3$, as well as the monodisperse case, $s_\sigma=0$, for reference. These quantities are seen to be relatively insensitive to the charge dispersion for the highly charged particles of the present sample. The effect of increasing polydispersity on the number-number distribution function $g_{NN}(r)$ is seen in Fig. 1 for $\rho\bar{\sigma}^2=0.15$. The general pattern of decreasing structure with increasing dispersion reproduces the behavior of polydisperse colloids in three dimensions.¹⁹ This is further mirrored in the number-number structure factor $S_{NN}(k)$, shown in Fig. 2. (The g_{NN} and S_{NN} curves for $s_\sigma=0.1$ are quite close to their monodisperse limits and are omitted in Figs. 1 and 2 for clarity.) The functions $g_{00}(r)-1$, $g_{10}(r)$, and $g_{11}(r)$ for correlations of density-density, size-density, and size-size fluctuations, respectively, Eqs. (21)–(23), are shown in Fig. 3 for density $\rho\bar{\sigma}^2=0.15$ and dispersion $s_\sigma=0.3$. We see, for example, that at the first peak of $g_{00}(r)$, which occurs at $r=2.54\bar{\sigma}$, the size-size fluc-

TABLE II. Computed thermodynamics of a polydisperse colloidal monolayer with Lennard-Jones potential of well depth $\beta\epsilon=0.25$ and Schulz distribution of relative standard deviation s_σ .

| $\rho\bar{\sigma}^2$ | s_σ | $\beta U/N$ | $\beta p/\rho$ | $\rho k_B T K_T$ |
|----------------------|------------|-------------|----------------|------------------|
| 0.2 | 0 | -0.0882 | 1.232 | 0.6468 |
| | 0.1 | -0.0887 | 1.234 | 0.6449 |
| | 0.2 | -0.0901 | 1.239 | 0.6389 |
| | 0.3 | -0.0926 | 1.247 | 0.6291 |
| | 0 | -0.1736 | 1.658 | 0.3459 |
| | 0.1 | -0.1745 | 1.665 | 0.3426 |
| 0.4 | 0.2 | -0.1775 | 1.688 | 0.3328 |
| | 0.3 | -0.1824 | 1.727 | 0.3168 |
| | 0 | -0.2383 | 2.541 | 0.1540 |
| | 0.1 | -0.2389 | 2.568 | 0.1510 |
| | 0.2 | -0.2408 | 2.651 | 0.1423 |
| | 0.3 | -0.2431 | 2.801 | 0.1287 |